Vulnerability Heatmapping in Debris Management

Richard G. Walker, S.M.ASCE[1]; Soojin Yoon, Ph.D., A.M.ASCE[2]; Anjin Chang, Ph.D.[3]; and Jinha Jung, Ph.D.[4]

Abstract: Debris generated and left in the wake of a disaster is one of a community's greatest obstacles in the ability to restore function. The objectives of this paper are (1) to provide systematic procedures to develop and visualize the vulnerability index (VI) based on three dimensions, and (2) to prioritize debris removal by integrating all dimensions into a geographic information system (GIS). The proposed methodology for vulnerability heatmapping consists of three dimensions: (1) physical, (2) infrastructure, and (3) environmental. An unmanned aerial vehicle (UAV) is used to quantify the debris three-dimensional (3D) volumetric information as part of the 11 metrics selected and evaluated to establish the vulnerability of a location. The proposed process incorporates all systems into a process to allow decision makers to quickly determine scope, complexity, potential impact, and recovery needs. Therefore, the outcome of this research will ensure maximum and timely utilization of limited resources to reach a greater number of people who might be facing life-threatening situations, enhancing the community's resilience. **DOI: 10.1061/JMENEA.MEENG-5507.**

Author keywords: Disaster response; Debris management; Process framework; Vulnerability index (VI); Data visualization; Hierarchical cluster analysis (HCA).

Introduction

A community consists of complex systems and inner workings that allow it to function and support a community. After a disaster, the systems that make up a community are susceptible to being impeded and unable to function. This hindrance is comprised primarily of the remnants of the disaster's destruction in the form of debris. The removal time of debris in a community's post-disaster response directly impacts the safety of a community's citizens, its environment, and overall function (Brown and Milke 2009). This becomes more crucial in scenarios such as Hurricane Katrina, where more than 100 million m^3 of debris was generated in the highly complex and variable environment of the New Orleans metropolitan area (Luther 2006).

In the disaster scenario, FEMA outlines the four phases of a disaster scenario: (1) mitigation, (2) preparedness, (3) response, and (4) recovery. The response phase, which takes place directly after a disaster occurs, is the phase that has the highest vulnerability (Paton et al. 2000). This is when a community is at the highest risk of potential effects of the disaster, with the most urgent need for safety and security. The response phase is also when potential long-term threats can be contained to have the least impact (FEMA 2017). To aid in restoring function, FEMA (2019d) outlined a list of the primary needed functions of a community postdisaster in the National Response Framework's (NRF's) seven community lifelines: (1) safety and security; (2) food, water, and shelter; (3) health and medical; (4) energy; (5) communications; (6) transportation; and (7) hazardous materials. FEMA's National Response Framework (FEMA 2019) focuses on relieving the points outlined by community lifelines and enables operations to increase the efficiency and effectiveness of incident stabilization, but does not give a defined response to disaster scenarios to guide the process.

Guidelines such as FEMA (2019) place greater importance on reestablishing communities' primary functions and give recommendations for prioritizing removal of debris postdisaster based on the priority of a situation's outcome, such as lifesaving and necessity. In the NRF, FEMA does not guide decision makers on implementing the given protocol or prioritizing similar events, leaving the situational guidance to the decision makers. Guidelines such as UN (2015) outline how disaster types can affect communities differently and the importance of planning and postdisaster response, but only give prioritization guidance by outcome type and do not offer guidance by individual factor. This is further shown in a review by the US Government Accountability Office (GAO 2016), which identified insufficient technology to develop protocols for addressing vital areas of disaster relief in areas such as functionality, processing, and information. All guidelines used for postdisaster response share the goal of protecting human life first and the community and environment second, so prioritization of debris will aim to promote a faster and more effective response.

There is currently an abundant number of guidelines (EPA 2019a, b, 2022; FEMA 2017, 2019a, b, 2020a, b; UN 2015, 2017) and decision makers involved in the disaster response process, but all lack a defined method for prioritization. This leaves many communities disorganized and panicked in the wake of disaster. The problem this study addresses is the current lack of a standardized and unified process specific to vital areas of disaster relief, which hinders the recovery of the community and can pose a heightened threat for long-term impact to the affected area. Therefore, there is a need to develop a systematic procedure for prioritizing the severity of debris postdisaster with the greatest emphasis on the response phase. This paper aims to provide a new methodology

[1]Ph.D. Candidate, Division of Civil Engineering, School of Civil and Environmental Engineering, Oklahoma State Univ., Stillwater, OK 74075. Email: grant.walker@okstate.edu

[2]Assistant Professor, Division of Engineering and Technology, Oklahoma State Univ., Stillwater, OK 74075 (corresponding author). Email: syoon@okstate.edu

[3]Associate Professor, College of Agriculture, Tennessee State Univ., Nashville, TN 37209. Email: achang@tnstate.edu

[4]Associate Professor, Lyles School of Civil Engineering, Purdue Univ., West Lafayette, IN 47907. Email: jinha@purdue.edu

Note. This manuscript was submitted on February 23, 2023; approved on November 6, 2023; published online on March 29, 2024. Discussion period open until August 29, 2024; separate discussions must be submitted for individual papers. This paper is part of the ***Journal of Management in Engineering***, © ASCE, ISSN 0742-597X.

to develop vulnerability heatmaps for prioritizing the removal of debris, in which the systematic procedure will lead to improvement of the disaster response process. The objectives of this paper are (1) to provide systematic procedures to develop and visualize the vulnerability index (VI) based on the three dimensions, and (2) to develop vulnerability heatmapping and an index for prioritizing debris removal by integrating all dimensions into a geographic information system (GIS).

The proposed methodology for a vulnerability heatmap consists of three dimensions, (1) physical, (2) infrastructure, and (3) environmental, comprising four layers, (1) physical, (2) civil, (3) civic, and (4) environmental. These dimensions and layers are used to define key areas of the response process and are represented by readily available metrics used to establish the severity of a debris impact on a location represented as vulnerability. For updated and accessible data, an unmanned aerial vehicle (UAV) will be used to collect data to map the spatial distribution of three-dimensional (3D) volumetric information and can be used to assess debris quantities and locations, and provide a platform for a GIS-based heatmap to be developed. The mapping and prioritization of debris locations using the VI will result in three primary heatmap designs: (1) dendrogram, (2) point, and (3) grid. The proposed VI with heatmap visualization will provide simplified information in multiple formats to suit situational needs, giving decision makers the ability to quickly determine scope and complexity and interpret the potential impact. This is done by instance prioritization by way of evaluating each location and assigning it a vulnerability value (VV) based on metrics. Also, clustering, which will group similar locations, helps prepare and organize by debris type based on locations sharing similar metrics. This framework will allow better decision management by stakeholders and a better structure of aid in the continued recovery effort, reporting, data collection, and predictive modeling.

Background

History of Debris Management

The response phase of debris management largely focuses on two primary metrics relating to measuring the severity of a postdisaster scenario: volume of generated debris and cost to remove the debris. Fig. 1 represents these two groups, showing the comparison of the quantities of debris generated by different types of disasters over time and how their removal costs correlate.

In Fig. 1, the *Y*-axis represents the value of both debris generated in millions of cubic meters and the cost of debris removal in billions of US dollars. On the *X*-axis is a chronological series of major natural disasters in the United States. Comparison of the two values by a scale of 1 million cubic meters of debris generated per unit to the disaster cost of 1 billion dollars per unit to remove gives an easier visual contrast of how the ratio differs from disaster to disaster. This gives a comparison of similar disasters such as Hurricane Katrina and Hurricane Harvey and shows that their cost of debris removal by volume differs widely. By contrast, the smaller disasters maintain a closer margin. Fig. 1 also shows a trend of the cost per million cubic meters decreasing over time. Further research into planning and preparation, as well as the collection of information and data, has led to a decrease in costs.

Current Guidelines for Disaster Debris Management

The use of predisaster planning has been shown to have an impact in reducing this cost, as well as the time required for cleanup (Crowley 2017). Predisaster plans are typically derived from government guidelines and research from the academic community but are ultimately derived by the decision makers using the plan. Examples used in this research, as well as what was taken and how it was applied, are listed in Table 1.

The guidelines directing the protocol are established by government bodies and cover a variety of protocols. Agencies set guidelines that cover all aspects of the disaster scenario through all phases and aspects of disaster response as listed in Table 1. Although guidelines for reporting to higher agencies are regulated, the development of response protocol is largely left up to the community to determine its preparedness plan according to environment type, community type, expected disaster type, and other region-specific decisions limiting the ability for a top-down protocol and specific framework for removal. FEMA's top-down guideline provides a clear and structured protocol for the highest priority instances that inform a vast number of the guidelines and manuals. FEMA also provides most of the reporting systems for additional aid and work to restore communities. UN and office for the

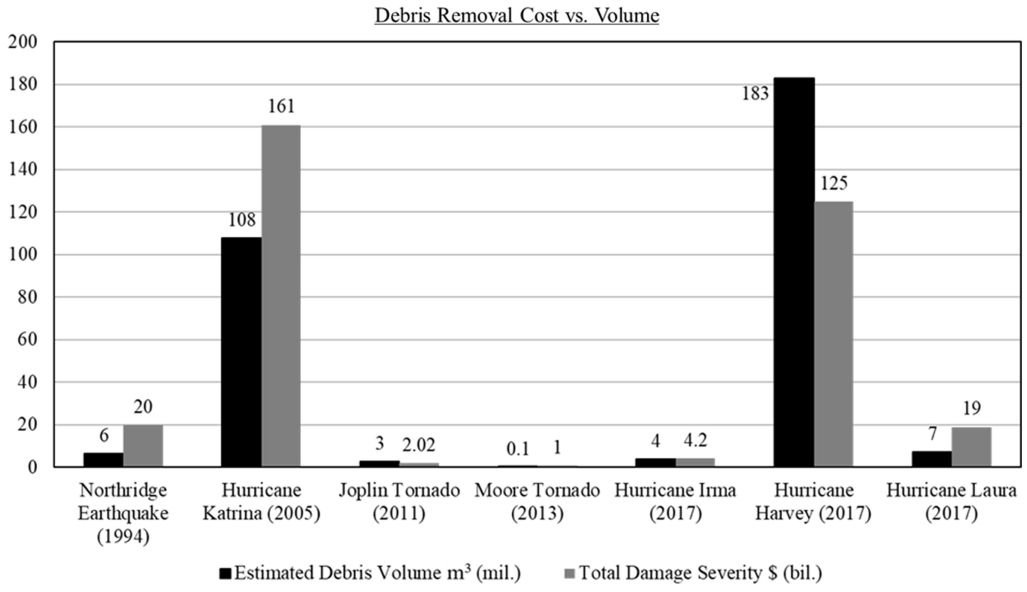

Fig. 1. Disaster volume versus severity (cost).

J. Manage. Eng., 2024, 40(4): 04024019

Table 1. Current guidelines for disaster debris management

Author	Type	Contents	Application
National Research Council (1994)	Guideline	Temporary debris management site (TDMS) recommendations Debris segregation Hazard ranking	Basis for EPA and DEQ evaluation systems. Shows framework of how Superfund Chemical Data Matrix Hazard Ranking System was developed and basis for hazard evaluation.
USAF (1999)	Manual	Government assistance plan Agency response protocol	Hazard recognition and debris handling. Military response protocol. Interaction with nongovernment organization protocol.
FEMA (2007)	Manual	Procedure and considerations for cleanup Optimization of TDMS	Debris groupings and removal teams. Outlines US procedure for removal and reimbursement. Outlines involvement of third-party contractors and organizations.
UNEP (2008)	Study	Case study Debris assessment Plan components	Debris management and grouping guide. Debris assessment forms and prioritization. Guidance on primary C&D waste.
FRCOG (2014)	Guideline	Planning guide Mapping overview Local specialization	Comprehensive reference for mapping elements such as TDMSs, routing, supply centers, key infrastructure, and vital civic systems.
UN (2015)	Study	Guidelines for risk reduction Emergency services Hazard warning and monitoring	Shows basic strategies of how to implement disaster risk reduction (DRR). Evolution of DRR and objective evolution. How disaster affects different communities.
GAO (2016)	Guideline	Deficiencies in FEMAs current information technology Areas of improvement Report vital functions	Addresses gaps in technology response protocol involving lack of functionality, low processing time, missing information, and lack of improvement.
FEMA (2017)	Guideline	Planning material Assistance recommendations Resource allocation	Dispersion of aid will be given to community through resources and proper funding protocol. Recommendations on debris reporting and resources allocation to aid in cleanup.
UN (2017)	Guideline	International protocol Debris segregation Current status	Guide used to assess debris and guide responders on protocol for cleanup. Acts as reference to predict environmental impact and gives environmental response protocol.
EPA (2019a)	Manual	Hazard recognition Management/handling Storage	Hazard mitigation and response planning. Community guidelines for how to structure response plans. Identify vital elements and resources.
FEMA (2019b)	Guideline	Resource allocation Financial and assistance planning Framework outline	Framework for FEMA's approach to disasters. Provides fundamentals such as grouping and third-party protocol. Gives planning advice such as vital structures, response capabilities, and stabilization tactics.
FEMA (2020b)	Guideline	Planning material Assistance Recommendations Resource allocation	Response and reporting recommendations and protocol. Coordination efforts across aid parties. Work grouping by debris types. Work procurement protocol. Operational priorities: community lifeline and action planning.

Note: DEQ = Department of Environmental Quality.

coordination of humanitarian affairs (OCHA) provide another subset of generalized guidelines, but also implement lessons learned in the form of case studies. Input detailing areas of deficiency often comes from organizations such as GAO. By providing post-disaster reports, as well as departmental reviews of how situations are handled, the GOA often reveal what is needed to improve in operation. While all guidelines provide necessary information on how to structure a community's procedure, the GAO shows that lack of cohesion and implantation of needed advancements have slowed potential progress in the area of disaster response (GAO 2016).

Current Research in Disaster Debris Management

Current disaster protocol research largely uses the guidelines and regulations set by the agency guidelines and manuals. Table 2 indicates a sample of the current research in disaster debris management research and objectives.

Much of the research focuses on performance reviews, showing gaps in process development and covering key advantages of disaster planning (Crowley and Flachsbart 2018; Marchesini and Barroca 2021), but does not define an implementable disaster protocol that can be used by a community. Much of the research has similar performance reviews—the focus of many is on predictive measures and how to better mitigate damage in specific divisions (Kim et al. 2018; Huang et al. 2021)—but fails to show integrations between key operation components to aid in community recovery. Other areas, such as sorting, removal, best practice, and optimization of recycling, are major priorities in the process (Lauritzen 2018; Marchesini and Barroca 2021) and are often represented but not in the form of the overall process. After reviewing current research, there is limited information regarding the overall process design involving different divisions, in which the entire phase process is evaluated with the goal of prioritization and optimization (Lorca et al. 2017).

Table 2. Current research in disaster debris management

Author	Deliverable	Application
Brown and Milke (2009)	Key issues in debris management	Key areas of focus in debris management. Highlights issues commonly found in organizational structure and decision-making.
Kim (2014)	Assessing debris removal	Highlights conditions for choosing the optimal sites for response. Gives protocol for assessing debris removal efficiency.
Lorca et al. (2015)	Scenario and procedure design	Resources needed to assist disaster and waste management officials with the collection, transportation, reduction, recycling, and disposal of debris.
Crowley (2017)	Key points in panning	Shows the effectiveness of a disaster relief plan by community type. Measures the effectiveness and efficiency of a preparedness plan. Recommendations and measurement of planning effects.
Lorca et al. (2017)	Scenario and procedure design	Outlines attributes for optimizing and balancing the financial costs, environmental costs, and duration of the collection and disposal operations.
Crowley and Flachsbart (2018)	Key points in planning	Analyze the extent to which debris management plans are complying with the FEMA policies that were established in the pilot program. Gives recommendations for planning.
Kim et al. (2018)	Key points in framework design	Framework for geographical information system and system dynamics to assess debris removal performance. Key points for outlining measurement protocol.
Lauritzen (2018)	Sorting and removal	Outlines general debris management practices. Gives tables, charts, forms, and other materials to aid in organizing and estimating cleanup.
Van Pham and Moore (2019)	Disaster decision modeling	Proposed sensibilities and preferences in emergency decision support. Decision analysis in dynamic uncertainty. Modeling using decision support systems.
Huang et al. (2021)	Prediction methodology	Importance of planning. Highlights and critiques the basis of the emergency management of unconventional emergencies. Outlines use of artificial intelligence and big data.
Marchesini and Barroca (2021)	Comparison of approaches to debris removal	Comparison of methods. Provides list of resources and data needed. Criteria on the precision and uncertainties of different approaches.
Guan et al. (2022)	Debris management and operations optimization	Key debris management grouping and process formatting. Decision planning and procedure optimization. Implementation of framework.

Although most areas of the process design have been researched, with a lack of specific research looking into a system that integrates all divisions of the disaster process, there remains a gap in research (Ford and Wolf 2020). Therefore, further research related to process design is needed to help stakeholders and communities evaluate and perform at a higher capacity to restore a community.

Methodology

The purpose of the research is to provide a framework to index and generate heatmaps of a disaster scenario showing the severity of its impact on an area. This can be used to show priority and guide the decision-making process in a disaster response scenario, as well as for guidance of debris removal routes and temporary debris management site (TDMS) selection. Fig. 2 represents the overall structure of the methodological process. As shown in Fig. 2, Phase 1 indicates the selection of dimensions to be evaluated applicable to the response phase. Phase 2 indicates the collection and processing of each category's metrics and associated techniques. Phase 3 indicates the process in which each metric used for the dimensions (Phase 2) is transformed using the method of standardization and combining the three layers. Phase 4 is to provide a vulnerability heatmap and the VI. The VI consists of two attributes: VV and grouping. The grouping is performed by hierarchical cluster

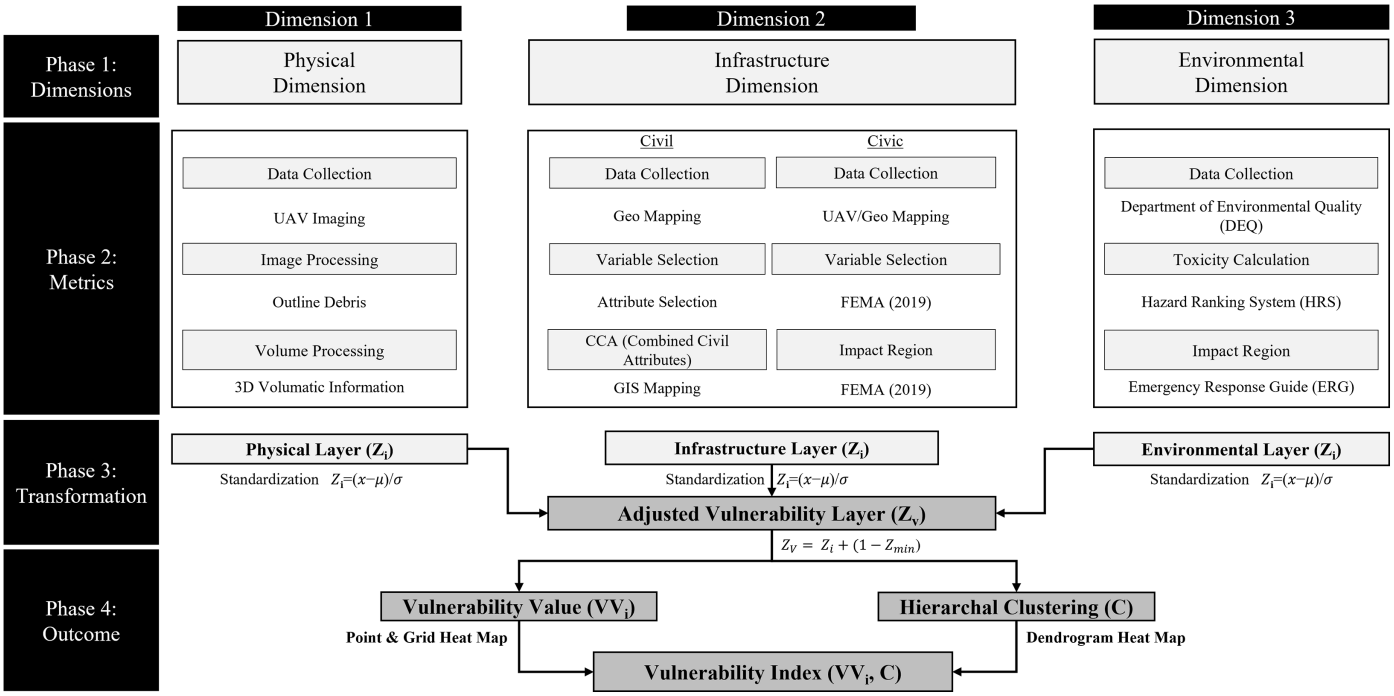

Fig. 2. Methodology process.

analysis (HCA). The detailed procedure for the methodology is as follows.

Phase 1: Dimensions

Three key dimensions were identified in the formulation of the methodology process. Dimensions were chosen on a basis like McNeill et al. (2006) and Kohlitz et al. (2020), grouping applicable metrics by similar attributes and decision makers. In the evaluation of key areas of vulnerability postdisaster, the National Response Framework's seven community lifelines act as the basis for continuing the operation of critical functions essential to human health and safety as well as economic security (FEMA 2019b).

One instance of debris, represented by the physical dimension, represents the location and volume of debris. This will be the primary metric and focus of the framework structure used in the evaluation. Its process will act as the collection point for impact data postdisaster, which will be used as the basis for the methodology process (Tran et al. 2020). The infrastructure dimension is made up of systems that control access and transportation of aid and emergency response. The dimensions encompass attributes highlighted by Boin and McConnell (2007), showing the importance of a cohesive response by decision makers. The environmental dimension includes risk factors related to exposure to hazardous chemicals and materials. The dimensions were created according to the EPA's identification of hazardous materials in emergency scenarios to mitigate exposure (Tseng et al. 2012).

Phase 2: Metrics

In Phase 2, dimensions are used as grouping for metrics, which are used to attribute values to be used to prioritize the locations that are highlighted as well as the process of evaluation. The evaluation metrics were selected by the availability and readiness of data collected by current data management tools, software, and catalogs commonly used by government agencies and decision makers. Metrics were based on the NRF seven community lifelines including safety and security; food, water, and shelter; health and medical; energy; communication; transportation; and hazardous materials (FEMA 2020b).

As shown in Table 3, the used metrics are periodized by dimensions and parameters using common measures and units to determine the potential vulnerability. Dimensions are further classified into parameters based on decision makers. The general dimension is added for grouping locations by attributes added in the evaluation process. The general category is not used in the framework because it is to only be used for database information. Parameters that fall within the same dimension category, as shown by the infrastructure dimension, are divided into the civil and civic parameters due to the overlap in controlling entities of the systems, as well as both assisting in postdisaster aid to infrastructure (Boyacı and Geroliminis 2012). From the parameters, the metrics are chosen for evaluation within each. Applicable parameters are chosen based on accessible and available data to be applied in the hierarchical process, such as volume for the physical dimension defining the cubic meters of debris in a location. The measures needed from these metrics are then defined for evaluation, and the appropriate unit is derived based on the formatting of the provider.

The general category represents all the variables assigned to debris locations needed for the database and the information for further analysis. This database information is used to sort and categorize all instances from multiple mapping types, such as map type point (P) or grid (G), and assigned location number (polygon).

Physical dimension is the basis of data collected in the methodology process. It is the only phase of the dimensions that will require active data collection at the time of the disaster. Shown in Fig. 3 are the three primary steps to the data collection process: data collection, image processing for 3D model development, and volumetric estimation. The data collection process shown is used for gathering the volume and location values (Yeom et al. 2019).

The data collection process utilizes UAV to take images of an area in a grid format. The grid format utilizes overlap (represented

Table 3. Dimension metrics used in vulnerability severity

Dimension	Parameter	Metric	Measure	Unit
General	—	Map type	Polygon/grid	Letter
		Polygon	—	Number
		Grid	—	Number
Physical	Debris	Volume	—	m^3
		Latitude	—	Number
		Longitude	—	Number
Infrastructure	Civil network	AADT	Value	Number
		Bridge	Number of lanes	Number
		Congestion	Value	0, 1, 2, 3[a]
		Airport	Flight number	Number
	Civic network	Hospital	Capacity	Number
		School	Capacity	Number
		EMT	Personnel	Number
		Fire	Personnel	Number
		Police	Personnel	Number
Environmental	Chemical type	Toxicity	Value	0, 1, 10, 100, 1,000[b]

[a]Unitless quantity.
[b]Proprietary unit used for measurement by agency.

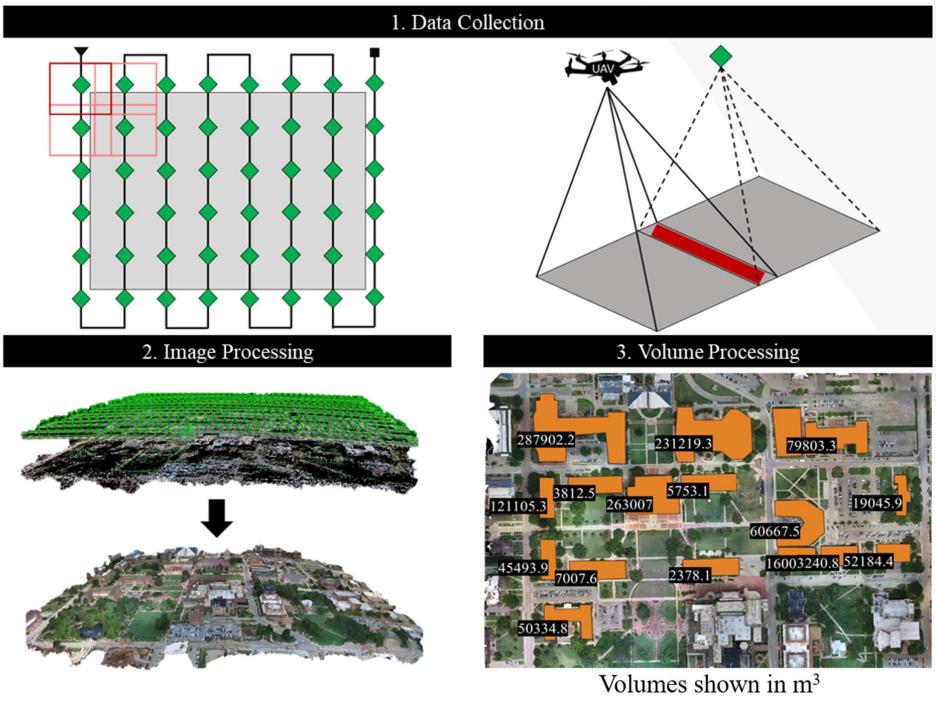

Fig. 3. Physical data collection process. (Images by Richard G. Walker.)

in "Data Collection") to ensure proper coverage of an area, which also creates a higher degree of accuracy (Siebert and Teizer 2014). With a series of captured images based on the grid format, each image has a property of geographically identifiable metadata. Using an inbuilt GPS linked to satellites for navigation, the UAV identifies the location when the picture is taken and stores the data in the file as metadata. The accuracy of the system shown by Da Silva et al. (2018) operates in a tolerance of 2.5–14.45 cm, with the variance defined by flight and camera parameters.

A photogrammetry software, Pix4D, is then used to generate various geospatial data products such as an orthomosaic image, digital surface model (DSM), and 3D point clouds. This process is known as structure from motion (SfM). SfM results in geospatial data products with measurable units, which enables direct estimation of volumetric information without field surveys (Siebert and Teizer 2014).

Civil and civic are correlating attributes, defined as resources needed to allow for transportation or evacuation or transportation of supplies and aid to a disaster area (FEMA 2019b). Therefore, the infrastructure dimension is classified into two layers: civil and civic. Civil is defined by the physical infrastructure, including average annual daily traffic (AADT), number of lanes, number of

flights at an airport, and severity of the congestion (TxDOT 2022). This is outlined by FEMA (2019b) as an essential system needed for the transportation of aid and personnel in and out of an affected area. Meanwhile, the civic layer is specified by essential facilities and emergency services in the community (FEMA 2019b). The metrics related to the civic layer vary according to the geographic size of the community and community population. The civic metrics define the necessary facilities in the community including the capacity of the school, the capacity of the hospital, the number of fire stations, the number of EMTs, and the number of police. The variables selected to be prioritized in the civic portion of the infrastructure dimension are outlined by FEMA (2019b) as essential services, as well as other areas that may act as suitable shelters or service areas.

The civil and civic data are collected first in the targeted area or community. These data can then be attached to a GIS as a point location marker or polygon of the structure provided by the municipality or available mapping service. The civic impact region shown in Fig. 2 indicates the region around a service that is required for the service to operate. This allows for defining an area that needs to be prioritized for cleanup so the service can operate at a maximum capacity based on the circumstances of the surrounding environment (Duhamel et al. 2016). Therefore, depending on the variable operation type and size, the buffer area can be adjusted for debris or hazard detection. On the other hand, once all metrics are selected in the civil layer, the attributes will be combined into a single layer that will represent all attributes. Unlike GIS mapping for the other dimensions, the civil layer has multiple attributes that are represented in different forms based on the data type. A process to merge and overlay these data is required to be able to transfer the attributes to the debris locations to establish severity.

Environmental dimension data collection is established by hazard waste guidelines from the Environmental Protection Agency (EPA 2019a). These registries act as a log of all locations containing hazardous materials in a region with various information on the material, location, storage type, and usage. The metric for the environmental dimension is toxicity classification. The toxicity class includes all toxicity and benchmark data used to determine human or ecotoxicity factor values. The value seen in Table 3 (0, 1, 10, 100, 1,000) represents the class of the toxicity of a material, with the larger number being more severe (EPA 2022). All agencies use factors in their registry that can be defined by the information in the Superfund Chemical Data Matrix (SCDM), which uses the Hazard Ranking System (HRS) (EPA 2022). The SCDM is used to generate a report with values based on the chemical type and conditions of the environment. This includes factor values, benchmarks, and data elements that can affect the potential toxicity of exposure and can be used to prioritize the potential impact of the hazardous material. Here toxicity is highlighted as the primary metric and is used to determine the impact region size by the proprietary value provided. Once the toxicity is calculated in the HRS, its defined safety distance and toxicity are given in the SCDM-HRS database (EPA 2022). The toxicity value establishes a severity ranking system resulting in an impact region to alert the potential presence of hazardous materials at a debris location (USDOT 2020).

Phase 3: Transformation

After the metrics have been applied, they are combined into a single layer comprising all attributes. Transformation allows for both individual analysis and the creation of a platform for all dimension layers to be merged into individual layers for comparison. Joining the layers then allows for comparison, but the method used to compare metric severity will need to be created as an unbiased system of evaluation based on individual disaster's metric severity.

Standardization of the data is needed for the comparison between data points due to the large variance between each metric unit, value, priority, and relative severity by disaster region (Hunter and Hamilton 2002). Before severity can be assessed, data transformation through the use of standardization is needed. The process of standardization of the original values using the standard score method requires the comparison of a single value versus all other values inside its metric category containing all locations. This process will give the relative severity of each metric in its category to be evaluated (Nevill et al. 2002). A comparison method that transforms based on severity among its metric category is used to determine the largest risk values (highest priority).

The standard score method was used to standardize the individual variables of all attributes to be used to permit comparison of metric severity; similar processes were used in other studies (Milligan and Cooper 1988; Truong and Somenahalli 2011; Yoon 2012). The Z-score converts the original data into values representing how many standard deviations a metric value of a location differs from the mean value in that category and is shown in Eq. (1), where x represents an observed value of an instance, μ represents the mean of the category, σ represents the standard deviation of the sample, and Z_i is the resulting standardized score of an instance metric

$$Z_i = \frac{(x - \mu)}{\sigma} \tag{1}$$

Other standardization methods, such as range scaling, which converts raw values to fit the scale [0,1] such as in Gupta (2013), have a limiting range of the scale used in distorting values when large outliers are observed, which skew the data. The unrestricted range of the standard score method allows for a clear representation of categorical difference by how far an instance's value is from other instances that share the same attribute, comparing how far its value differs from the mean value [0] (Patro and Sahu 2015). Therefore, this research would transform the data by adjusting the values as given in Table 4. Taking the value (x) and subtracting the category mean (μ) for the volume category, then dividing the result by the standard deviation (σ) of the category gives the standardized Z-score of the original value.

Because the results of the standardization include negative values, the scaling and rescaling processes are required to return the negative values of the standardization method to usable values. Brock (2018) showed the application of rescaling used in evaluating T-scores and IQ testing (Sansone et al. 2014). Eq. (2) indicates the scaling method basis and Eq. (3) represents the rescaling used in the process. The scaling is performed by the scaled scoring method,

Table 4. Example standardization

Parameter	Volume	AADT	Bridge	Congestion	Airport	EMT	Fire	School	Police	Hospital	Toxicity
Value (x)	135	2,310	4	0	1,524	0	0	0	0	0	10
Metric mean (μ)	148.78	24,616.9	2.5	0.05	29.09	0.44	0.42	73.5	1.25	1.5	23.5
Standard deviation (σ)	79.66	29,177.15	1.45	0.30	203.87	1.97	1.83	242.53	10.23	14.92	32.14
Standardized (Z_i)	−0.173	−0.765	1.033	−0.169	7.333	−0.224	−0.229	−0.303	−0.122	−0.101	−0.420

Table 5. Example rescaling [adjusted Z vulnerability layer (Z_V)]

Parameter	Volume	AADT	Bridge	Congestion	Airport	EMT	Fire	School	Police	Hospital	Toxicity
Standardization	−0.173	−0.765	1.033	−0.169	7.333	−0.224	−0.229	−0.303	−0.122	−0.101	−0.420
Metric minimum value ($Z_{\min}$)	−1.805	−0.844	−1.721	−0.169	−0.143	−0.224	−0.229	−0.303	−0.122	−0.101	−0.420
Adjusted mean $1 - (Z_{\min})$	2.805	1.844	2.721	1.169	1.143	1.224	1.229	1.303	1.122	1.101	1.420
Z vulnerability value (Z_V)	**2.632**	**1.079**	**3.754**	**1.000**	**8.475**	**1.000**	**1.000**	**1.000**	**1.000**	**1.000**	**1.000**

Note: Bold values represent the finalized values used for the vulnerability calculation.

finding the mean value (μ) and standard deviation (σ), then multiplying the Z_i with the standard deviation (σ) and adding it to the adjusted mean (μ), resulting in Eq. (2) (Nkikabahizi et al. 2022)

$$Z_{\text{adj}} = \mu + (\sigma \times Z_i) \tag{2}$$

$$Z_V = Z_i + (1 - Z_{\min}) \tag{3}$$

The rescaling is formatted by fixing the minimum values (Ismail Bin and Dauda 2013; Schwab et al. 2020). This is done by setting the minimum value at 1 which is done by subtracting the minimum standardized value ($Z_{\min}$) from 1 then adding it to the initial Z score (Z_i) in the category gives our resulting adjusted Z vulnerability value (Z_V), shown in Eq. (3). This will change the mean from 0 for the category to what value is needed to add to change the minimum standardized value to 1. Table 5 indicates the value transformation from standardization to the adjusted value (Z_V) continued from Table 4.

The parameter minimum, which gives the value by which the scale will need to be adjusted, will give the change needed to each variable to get the minimum to 1. The amount of change needed for all is reflected by the adjusted mean, which was originally 0 from the standardization. This adjustment can be seen based on the values in the category that change the standardized value to the Z vulnerability value. Therefore, in Table 5, the resulting Z_V shows the severity of that location's attributes in comparison to the rest. The minimum value, which means that the attribute is not represented in a location, is reflected by a "1" for the Z_V. As we can see in Table 5, values above 1 would reflect that that metric is present at the debris location and would increase the location's severity value. The more the value increases, the higher the location's severity. In the example, we can see that the airport would be a much more impactful value, making the debris in that location more detrimental, possibly due to a limited number of airports, and more so than the AADT with a low severity value reflecting that it is a low-trafficked road.

Phase 4: Outcome

The vulnerability value (VV_i) of an instance is then calculated based on the aggregation of all its variables that have now been standardized to show its categorical severity. The vulnerability value VV_i implies a composite index consisting of three dimensions (physical, infrastructure, and environmental) to monitor the severity of the vulnerability of all instances in a community or state postdisaster to facilitate data-driven decision-making. Therefore, the proposed VV_i can be implemented to present the volatility of the disaster.

The geometric mean uses the process of multiplying all values together and taking the nth root of the result (Das et al. 2019) to develop the VV_i. This process will be used in combining the transformed metrics within a dimension, as well as combining the dimensions of an instance [Eq. (2)]. The resulting mean signifies the central tendency of the set of numbers by finding the product of their values. This allows for the reduction of compensation among the other dimensions but allows for decision makers to trace roots of the normalized attributes (Bhattacharyya et al. 2021; Jeon et al. 2021). These are the given advantages compared with using other methods such as the arithmetic mean. Cross comparison of categories using the geometric mean can skew data, but in the case of normalized metrics, the aggregation preserves the scaled severity of each instance in comparison with the sample population (Barzilai et al. 1992). With needing for a proprietary measure to place greater weight on a single dimension, the geometric mean formula was altered to fit the criteria evaluation required, shown in Eq. (4)

$$\text{VV}_i = P \times (C_1 \times C_2 \times E)^{1/3} \tag{4}$$

The VV_i is used to calculate the severity of vulnerability of an individual instance. This equation acts as a representation of each dimension, or parameter for larger dimensions, in the calculation of risk severity of a location. Each part of the formula represents the summation of attributes of each dimension, with physical represented by P, both parameters of the infrastructure dimension represented by C_1 for civil and C_2 for civic, and the environmental dimension represented by E. With the physical P being the focus attribute used for evaluation in this example, the formula is structured so it has a greater weight than the others on the calculation. The VI will serve as the primary aggregation metric of severity of the vulnerability of a location's attributes.

From the example outcomes found in Table 6, the VI would be established by summing the normalized value of Polygon 1. Using Eq. (4), the resulting formula for Polygon 1 to establish its VV_i is

$$(2.632) \times ((1.079 \times 3.754 \times 1 \times 8.475)^{1/4} \times (1 \times 1 \times 1 \times 1 \times 1)^{1/5} \times (1))^{1/3} = 1.506$$

The resulting vulnerability value is 1.506. In comparison with the other observed values, this would reflect as the third most severe vulnerability and location, with Polygon 2 being the most severe at 2.125, and Polygon 5 being the least severe at 0.9.

Point heatmap and grid heatmap use two types of data visualization, the first showing the severity of a singular metric, and the second by use of the vulnerability values. The point map is used to show the severity of a single attribute in comparison to the rest of the population by displaying the severity per instance (Chen and Yang 2020). This provides the most accurate geographical representation of the data and its severity in an area as shown by Fahad et al. (2022). The grid heatmap is divided by a set area to highlight regions within an evaluation area that may be affected differently than the surrounding. By combining all normalized attributes and dividing locations into a grid, the attributes inside each grid can be combined to find which zone was more affected, much like the point heatmap (Flenniken et al. 2020). The grid heatmap can also represent which metric may be affecting an area disproportionately high, as well as display an outlier subregion that may not be seen by looking at individual locations (Liu et al. 2021).

Clustering is the process of identifying similar groups of variables on selected attributes. It acts as a similarity measure by defining the number of groups (k) that will then define each grouping of

Table 6. Example transformed data

Polygon	Volume	AADT	Bridge	Congestion	Airport	EMT	Fire	School	Police	Hospital	Toxicity	VV
1	2.632	1.079	3.754	1.000	8.475	1.000	1.000	1.000	1.000	1.000	1.000	1.506
2	2.644	3.625	3.754	1.000	1.000	3.543	1.000	1.000	1.000	1.000	1.000	2.125
3	2.657	4.458	2.377	4.381	1.000	1.000	1.000	1.000	1.000	1.000	1.000	2.056
4	2.770	1.111	3.754	1.000	1.000	6.086	1.000	1.000	1.000	1.000	1.000	1.171
5	3.360	1.111	2.377	1.000	1.000	6.086	1.000	1.000	1.000	1.000	1.000	0.900

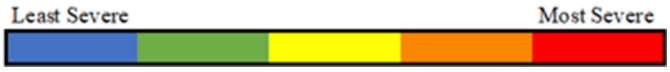

Fig. 4. FEMA severity matrix. (Reprinted from FEMA 2020a.)

instances by like-attribute severity. Although prioritization serves the purpose of showing severity, in many cases the optimal format is to group instances by like characteristics (Charrad et al. 2014). The chosen method for grouping and ranking the severity of a location is based on HCA. HCA was chosen for the clustering design, which is shared with other methods like *k*-means clustering, is less susceptible to outliers, and provides a hierarchical rank (Violán et al. 2018).

When performing HCA, there are three primary attributes to be determined that are used to define the clusters and their relations: (1) the distance method, (2) the linking method, and (3) the number of clusters. The distance method uses dissimilarities in the individual attributes of a location to determine the distance between objects (instances) when forming clusters (Saraçli et al. 2013). The distance represents how much the two instances differ, shown on a dendrogram by being farther away and having a higher distance value, or how much their characteristics are alike by being closer with a lower difference in distance value. The linking method then uses dissimilarities among attributes in groups to calculate how much attributes differ from other instances by finding how much each location's variables differ; this determines the clusters for the clustering hierarchy (Murtagh and Contreras 2011). There are multiple methods for each distance and linking method, but they often require changing based on the variance and type of data (Nielsen 2016). The distance and linking chosen here will be by which combination of methods provides the highest cophenetic correlation coefficient, which shows the goodness of fit for the cluster, based on the linking and distance combination (Saraçli et al. 2013; Carvalho et al. 2019). This method allows for the best distance and linking methods to be used to link the variables, giving the best possible fit for the division of attributes into clusters.

The third attribute used to define the clustering is the number of clusters (k). There are five classes used ($k = 5$) in this process based on FEMA's five-tier severity ranking shown in Fig. 4. By changing the number of clusters, the outcome will still group into the desired number of clusters by which attributes share like characteristics and severity. This is represented with a spectral color palette reflecting the least severe to most severe values: blue, green, yellow, orange, and red (FEMA 2020a).

The clusters are represented by a dendrogram, shown in Fig. 5 which uses a tree to show the closeness of relation between instances. The lower the difference in distance value of two given branch heights, the closer the two instances are related (Forina et al. 2002). As can be seen in Fig. 5, when clustering instances, the dendrogram is grouped by tracing the branches down to divide where the group can be split into two different clusters. This can be traced down until the needed number of clusters is reached. In the case of creating the next set of clusters, the first cluster is split, and the assignment is removed as shown by the asterisk. The next closest branch moving down the tree would define the next two clusters.

A dendrogram heatmap is a representation of the data's attributes in a clustered format (Gu 2022). This is used to cluster each location into classes, as defined by the user matrix, so that groups of locations with similar characteristics can be identified. This also allows for the evaluation of the location's severity by individual metric category, allowing for the identification of the instance's

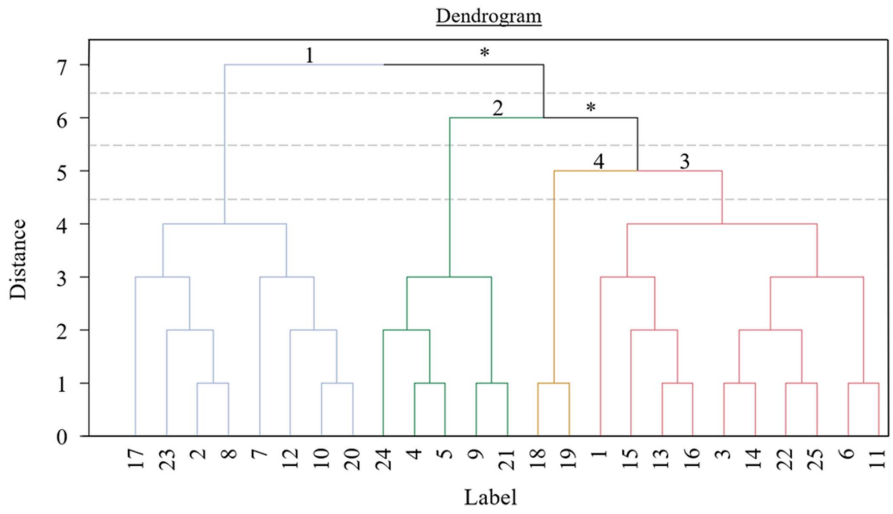

Fig. 5. Example dendrogram.

Table 7. Disaster area information

Area	Area (km^2)	Population	Debris estimate (m^3)	Damage costs (USD)
Hurricane Harvey	37,014 (Blake and Zelinsky 2018)	738,000 (Amadeo 2019)	152,910,971 (Amadeo 2019)	125,000,000,000 (Blake and Zelinsky 2018)
Corpus Christi	259 (USCB 2020)	317, 863 (USCB 2020)	344,050 (FEMA 2019)	12,000,000 (FEMA 2019)
Holiday Beach	3 (USCB 2010)	514 (USCB 2020)	52,854 (TCS 2017)	587,294 (TCS 2017)

metrics risk (Gu et al. 2016). An example of this including the use of the dendrogram is given in Table 7. The heatmap's dendrogram is shown on the left *Y*-axis, with one row representing the metrics of a debris location. Using the color scale to reflect their categorical severity, the metric category is represented on the *X*-axis. This shows the transformed data that led to the attribute severity types showing locations with like attributes. The proposed heatmaps will incorporate and display all metrics into a heatmap to allow effective and efficient planning by entities responsible for emergency coordination as shown in de Brito Neto (2015). In this research, the three heatmaps provide decision makers varying formats for viewing the data, according to operational needs. As given in Table 7, the features and outcomes of the maps have different purposes, such as the analysis of categorical severity in the dendrogram map versus the location severity in the point and grid maps. The heatmaps also show similar data in varying formats as shown by the grid and point heatmap, allowing each to suit the situational needs of the user.

Data collection and processing of increasingly large and complex data sets pose a difficulty in how decision makers are to understand and use the information (Gu 2022). Data visualization provides a platform for a greater understanding of a data set's characteristics (e Silva et al. 2021). A heatmap, as a result, provides decision makers with greater means of data visualization for an affected community. This visualization presents data in a way that can be used to find the most severe individual locations, outliers, patterns, isolated high-impact areas, and attributes with the greatest effect.

This research provides not only visualized heatmapping, but also indexing by way of the VI. The VI is a tool used to aggregate and display data to find trends, projections, patterns, and dynamics (Naderpajouh et al. 2016; Yoon et al. 2021). The vulnerability index is defined by two attributes: (1) vulnerability value; and (2) clustering. Eq. (6) indicates the formation of the vulnerability index

$$\text{Debris Vulnerability Index}(\text{VV}_i, C) \tag{5}$$

The vulnerability value (VV_i) is a composite value combining all metrics with all dimensions using the geometric mean. The severity is represented by way of the vulnerability value, which acts as the key metric for prioritization. This acts as a clear indicator for comparison of the vulnerability of all debris locations. The clustering (C) indicates the cluster assigned to the instance. HCA was conducted to create the clustering so that groupings of similar locations can be identified. When paired with the VV, this will allow decision makers to see the most vulnerable locations by similar types. Combining both metrics in one index allows decision makers a clearer representation of priority in a more direct format.

Case Study

The proposed framework was applied to the case of Hurricane Harvey in Texas to validate the methodology process. The validation was mainly performed with two processes: (1) a volume analysis of collected data, and (2) a simulation of the process on a more complex area containing all attributes. The locations of the case study take place in two areas of southeast Texas on the Gulf of Mexico, (1) Holiday Beach; and (2) Corpus Christi.

The scope of evaluation for the case study consisted of approximately 3 km^2 (2 mi^2) of the Holiday Beach community and 129 km^2 (80 mi^2) of Corpus Christi. Additionally, Table 8 displays the estimated total amount of area impacted, population affected, debris generated, and cost of removal and repair of Hurricane Harvey's total damage and its impact on the scope area. The total damage cost of Hurricane Harvey is estimated at USD 125,000,000,000, while USD 12,000,000 is estimated for Corpus Christi and USD 587,294 is estimated for Holiday Beach.

Phase 1 and Phase 2: Metrics

The research applied the three dimensions (physical, infrastructure, and environmental) in Phase 1. UAV mapping missions were conducted after Hurricane Harvey in Phase 2 to collect the data and establish the proposed metrics. Harvey affected south-central Texas from August 25 to 29, 2017, and Holiday Beach was directly hit on August 26, 2017. For the UAV mission, we had to consider weather conditions and postdisaster issues, such as potential public health problems caused by floods, accessibility to Holiday Beach, and local security. After addressing all the issues of accessing Holiday Beach surrounding safety and objective, data collection began 2 weeks postdisaster by the Texas A&M, Corpus Christi team. UAV data of the Holiday Beach area were taken in monthly increments of the area to quantify debris volumes. A DJI Phantom 4 (Holiday Beach, Lebanon) was used to capture the data at a flight altitude of approximately 61 m (200 ft) above ground. The polygons outlining the debris locations were added manually and evaluated for volume as shown in Fig. 6. The physical dimensions of Holiday Beach were then applied to the Corpus Christi area. Using QGIS's randomized point generator, randomized volumes scaled to the same distribution as Holiday Beach were used in the case study. Fig. 7 displays two maps that act as the GIS representation of the physical dimension. The two maps shown represent (A) Holiday Beach Heatmap of Debris Volume and (B) Corpus Christi Physical Layer. As can be seen from Fig. 7(a), the Holiday Beach Heatmap of Debris Volume was calculated for the location. Fig. 7(b) shows the result of the simulation of the physical layer in Corpus Christi, where the debris points were distributed randomly throughout the evaluation area. This acts as the basis for points of contact for the application of the other dimensions.

The civil and civic parameters of the infrastructure dimension represent metrics of the community needed to provide aid. The civil data were taken from the Texas Department of Transportation's (TxDOT's) open data portal (TxDOT 2022). Each metric was individually grouped and needed to be packaged into a single layer as shown in Fig. 8. A buffer was applied to ensure the region covered all access points and was expanded around roadways and critical infrastructure points. The civic portion of the infrastructure dimension utilized OpenStreetMap (OSM) locations to find the locations of each metric in Corpus Christi. By using the characteristics, such

Table 8. Results of standardization

Transformation	Polygon	Volume	AADT	Bridge	Congestion	Airport	EMT	Fire	School	Police	Hospital	Toxicity
Raw data	6,339	193	3,230	2	0	0	10	0	0	0	0	10
	13,456	119	8,384	2	2	0	0	0	0	0	0	10
	22,647	136	76,597	4	0	0	5	0	0	0	0	10
	49,037	102	41,820	2	0	0	0	0	0	100	0	10
	57,924	125	43,210	2	0	0	9	0	0	0	0	10
	60,509	262	3,230	2	0	0	10	0	0	0	0	10
	69,444	135	2,310	4	0	1,524	0	0	0	0	0	10
	103,651	44	40,090	2	0	1,385	0	0	0	0	0	10
	108,046	146	3,230	4	0	0	10	0	0	0	0	10
	112,311	137	100,900	2	1	0	0	0	0	0	0	10
Standardization	6,339	0.555	−0.733	−0.344	−0.169	−0.143	4.862	−0.229	−0.303	−0.122	−0.101	−0.420
$Z_i = (x - \mu)/\sigma$	13,456	−0.374	−0.556	−0.344	6.592	−0.143	−0.224	−0.229	−0.303	−0.122	−0.101	−0.420
	22,647	−0.160	1.782	1.033	−0.169	−0.143	2.319	−0.229	−0.303	−0.122	−0.101	−0.420
	49,037	−0.587	0.590	−0.344	−0.169	−0.143	−0.224	−0.229	−0.303	9.651	−0.101	−0.420
	57,924	−0.299	0.637	−0.344	−0.169	−0.143	4.353	−0.229	−0.303	−0.122	−0.101	−0.420
	60,509	1.421	−0.733	−0.344	−0.169	−0.143	4.862	−0.229	−0.303	−0.122	−0.101	−0.420
	69,444	−0.173	−0.765	1.033	−0.169	7.333	−0.224	−0.229	−0.303	−0.122	−0.101	−0.420
	103,651	−1.315	0.530	−0.344	−0.169	6.651	−0.224	−0.229	−0.303	−0.122	−0.101	−0.420
	108,046	−0.035	−0.733	1.033	−0.169	−0.143	4.862	−0.229	−0.303	−0.122	−0.101	−0.420
	112,311	−0.148	2.614	−0.344	3.212	−0.143	−0.224	−0.229	−0.303	−0.122	−0.101	−0.420
Scaling	6,339	3.360	1.111	2.377	1.000	1.000	6.086	1.000	1.000	1.000	1.000	1.000
$Z_V = Z_i + (1 - Z_{\min})$	13,456	2.431	1.287	2.377	7.761	1.000	1.000	1.000	1.000	1.000	1.000	1.000
	22,647	2.644	3.625	3.754	1.000	1.000	3.543	1.000	1.000	1.000	1.000	1.000
	49,037	2.218	2.433	2.377	1.000	1.000	1.000	1.000	1.000	10.774	1.000	1.000
	57,924	2.506	2.481	2.377	1.000	1.000	5.577	1.000	1.000	1.000	1.000	1.000
	60,509	4.226	1.111	2.377	1.000	1.000	6.086	1.000	1.000	1.000	1.000	1.000
	69,444	2.632	1.079	3.754	1.000	8.475	1.000	1.000	1.000	1.000	1.000	1.000
	103,651	1.490	2.374	2.377	1.000	7.794	1.000	1.000	1.000	1.000	1.000	1.000
	108,046	2.770	1.111	3.754	1.000	1.000	6.086	1.000	1.000	1.000	1.000	1.000
	112,311	2.657	4.458	2.377	4.381	1.000	1.000	1.000	1.000	1.000	1.000	1.000

Feature	Dendrogram Heatmap	Point Heatmap	Grid Heatmap
Features	Dendrogram and map represent categorical severity of debris location. Cluster by attributes showing relation.	Point heat map showing severity by instance location. Displays most accurate representation of metric severity.	Grid heatmap displaying severity of combined attributes broken up by grid. Cumulative severity by zone.
Map Figure	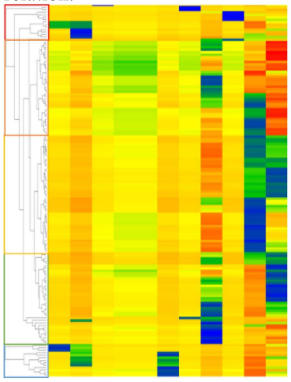		
Outcome	Represents severity of variables in comparison of metric category.	Shows VV and metric severity by individual instance.	Shows summed VV and individual metric severity by a 10x10m grid.

Fig. 6. Heatmap summary table.

as facility type or capacity, a buffer was set around all locations acting as the impact region, shown in Fig. 8.

The environmental dimension uses the toxicity numbers of the SCDM to establish the impact region of the environmental layer (EPA 2022). Hazard registry information is held by government officials and is not available for outside use. Therefore, a random point generator was used to add locations for the simulation, shown in Fig. 8. Values were randomly assigned, based on a right skew, and a buffer that acts as the impact region was added based on the toxicity value.

Phase 3: Transformation

The purpose of the transformation is to prepare the data in its raw format to a representation that can be used for analysis by the vulnerability value equation. The transformation process consists of two processes: (1) standardization; and (2) scaling. The standardization is transformation of raw values to a standard value on the same scale (Z-score). Scaling is the process of moving the represented data to a new set of values but maintaining the integrity of the data, so it represents the same data. Fig. 9 indicates a part of the results of the standardization and scaling process. The columns in Fig. 9 represent the metrics used for evaluation. Table 8 indicates a part of the result of the standardization and scaling process. The columns in Table 8 represent the metrics used for evaluation. The rows represent the three steps of the transformation process: (1) raw Data, (2) standardization, and (3) scaling. The raw data show 10 debris locations from the simulation and their associated metric values. The standardization of the raw data was performed by using Eq. (1), standardizing the raw data values by Z-score. Scaling the attributes further by using Eq. (3), the data were rescaled to set the minimum value of each metric category to 1, showing the increasing severity of metrics with greater values.

As can be seen from Fig. 9, it is revealed that the transformation process applied to 10 instances from a larger data set and how the values are affected. These data are to be used in the process to evaluate and combine the data by vulnerability value. The VV score, as shown by Eq. (4), uses the geometric mean. Due to the calculation of a geometric mean, transformation is needed to set null values of metrics found in locations to a value that does not affect the result. The calculation also requires the implementation of a standard in the evaluation of metric comparison so there is a standard set for the comparison of metric severity; this is done by standardization. In the scaling process, the values are adjusted to represent the data set while setting the minimum value at 1. This result can be seen more clearly by comparing the transformed values in the scaling section to the initial values in the raw data section. Therefore, this outcome value is the base that provides the values to calculate the VV, which is then reflected further through visualization by heatmapping and indexing of the locations to rank and cluster for the outcome.

Vulnerability Layers are used to combine all dimensions to form a cohesive GIS map, that contains the data and can then be used for the analysis process, shown in Fig. 9. This is the outcome of the GIS tool (QGIS) used to overlay the data collected for evaluation. Its purpose is to create a virtual representation of the data so that geospatial attributes, primarily location, can be used to find the points of interaction. Shapefiles were used to create the virtual representation while also containing the physical attribute data.

Each layer was constructed in GIS, giving the attributes a virtual representation. This process is where the virtual layers are combined to find if a debris location contacts any attribute found in the other layers (Fig. 8). Any resulting contact is reflected by applying that metric to the debris location (polygon). Additionally, in Fig. 7 there are more than 130,000 debris locations represented by the black dots. Each time another attribute, shown by the colored shapes, comes into contact with a debris location, its data are added to the debris location's shapefile attributes. This is the visual outcome that comes alongside the process of combining the data, represented in Fig. 9.

Phase 4: Outcome

The outcomes of the debris management with vulnerability heatmap are (1) the development of VV to measure the severity post-disaster, and (2) visualization of the vulnerability by providing heating maps (dendrogram heatmap, point heatmap, and grid heatmap). Fig. 10 shows the result of the simulation heatmap of the case

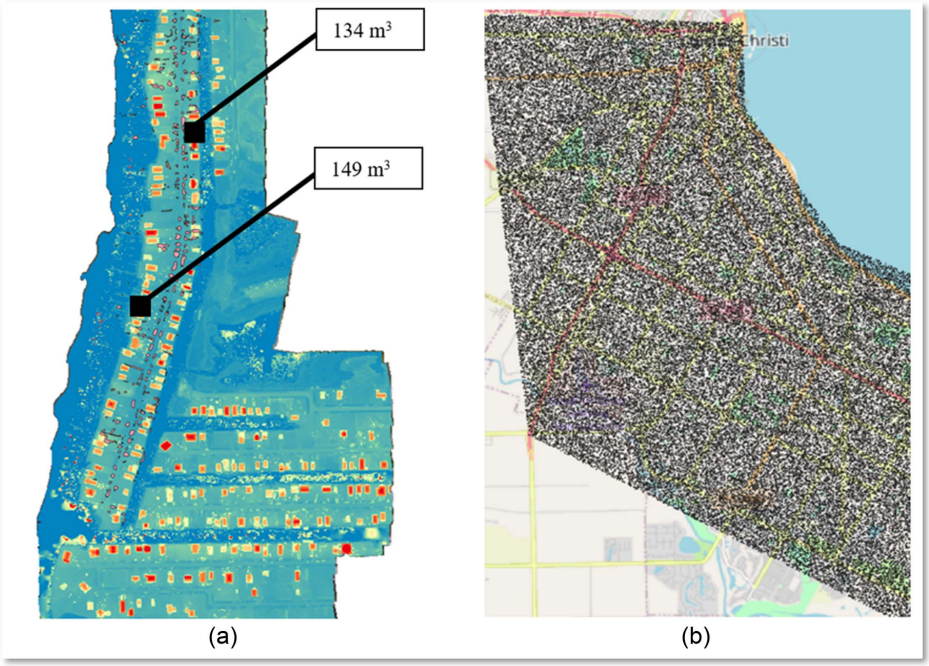

Fig. 7. Physical layer for case study: (a) Holiday Beach heatmap of debris volume; and (b) Corpus Cristi physical layer. (Base map © OpenStreetMap contributors.)

Dimensions	Infrastructure		Environmental
Parameters	Civil	Civic	Chemical Type
GIS Simulation Results	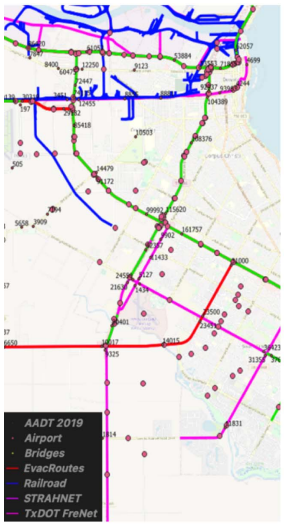	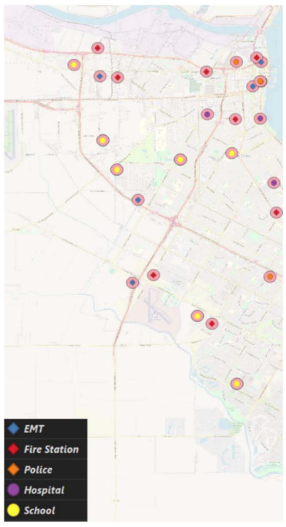	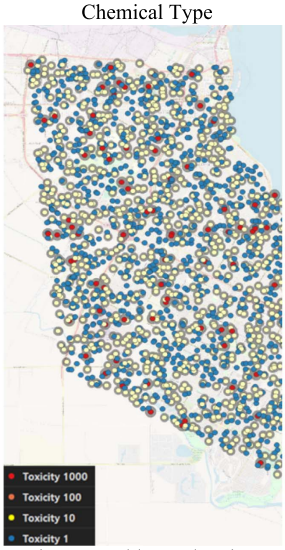
Outcome	Civil layer showing transportation attributes.	Civic layer showing impact region of service facilities.	Environmental layer showing impact region by toxicity.

Fig. 8. Individual layer results. (Base map © OpenStreetMap contributors.)

study. The point heatmap shows individual locations representing the VV in Corpus Christi. The study allows five classes used ($k = 5$) based on FEMA's five-tier severity ranking, including blue, green, yellow, orange, and red (FEMA 2020b). Red indicates high severity, while blue indicates low severity of the VV. The grid heatmap represents the zone-based VV in Corpus Christi. The heatmap implies severity values in a 100×100 m zone compiled to show zone severity. The severity is expressed in color as shown in the point heatmap. Additionally, the grid map serves a similar function to the point map by displaying the same data but aggregated further. This visualization method works for the evaluation of the data in a way that shows areas of greatest need and helps reduce the effect of outliers.

The VI is the final deliverable to show not only the vulnerability postdisaster (vulnerability value) but also location categorization (cluster). The clustering is visualized by the dendrogram. Fig. 11

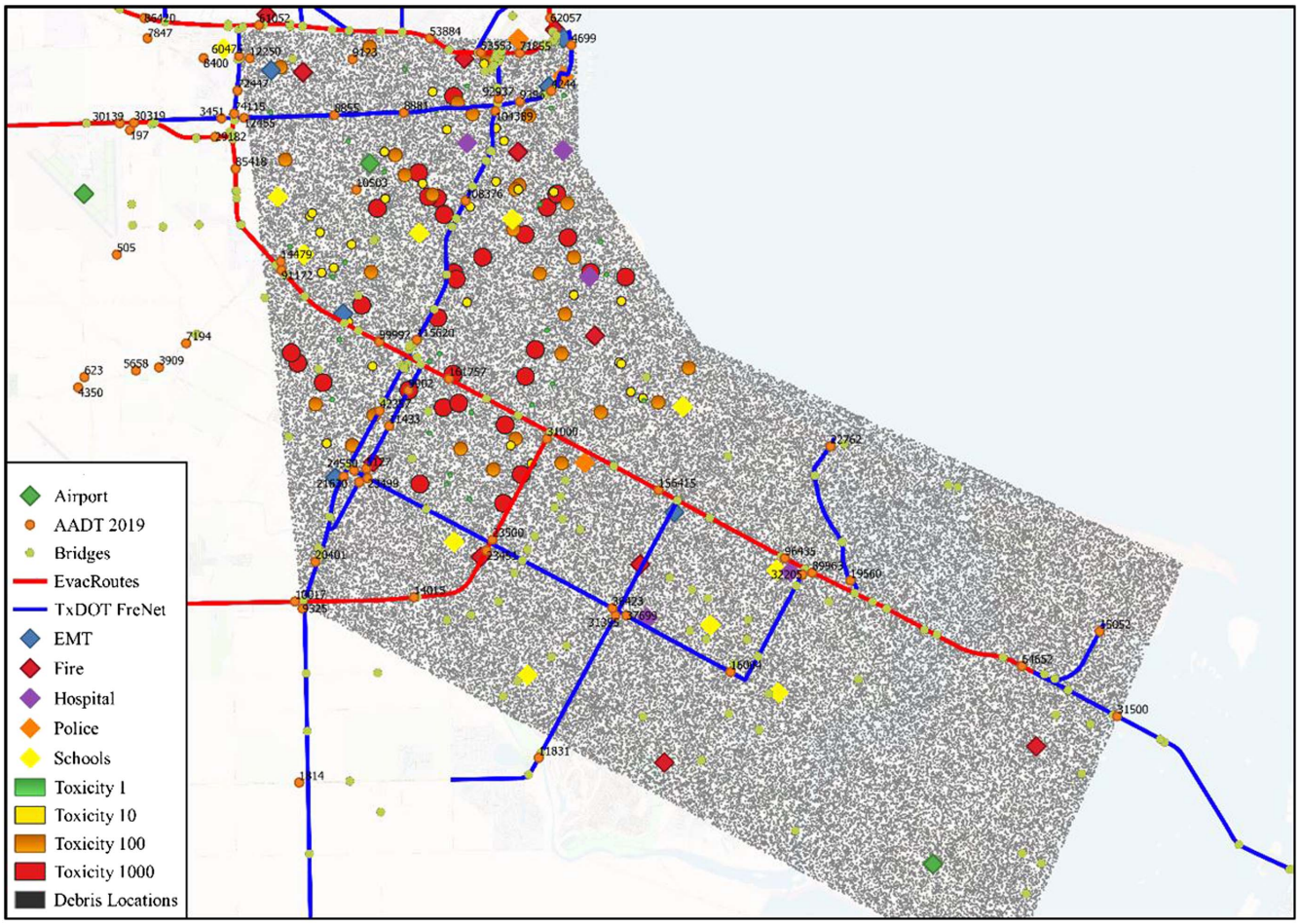

Fig. 9. Combined layers. (Base map © OpenStreetMap contributors.)

Feature	Point Heatmap	Grid Heatmap
Description	Heatmap of individual locations representing the VV in Corpus Christi.	Heatmap of zones representing the compiled VV in Corpus Christi.
Map Figure	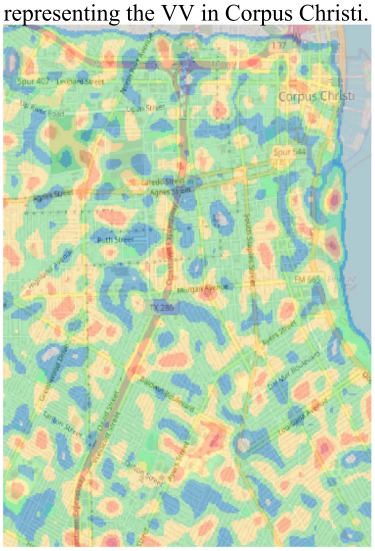	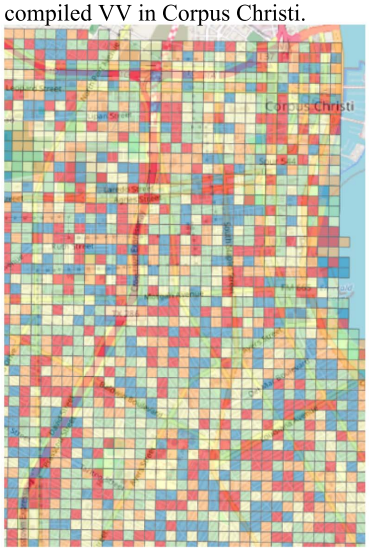
Outcome	Point heat map showing severity by instance. Best visual representation of conditions of severity.	Grid map showing severity values in a 100x100 meter zone compiled to show zone severity.

Fig. 10. Simulation heatmap results. (Base map © OpenStreetMap contributors.)

	Polygon	VV	Cluster	Dendrogram
Results VI (VV, C)	6339	0.900	1	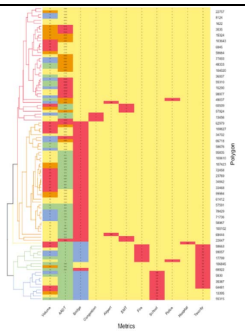
	13456	0.962	1	
	22647	2.125	2	
	49037	2.303	1	
	57924	1.374	2	
	60509	1.132	1	
	69444	1.506	3	
	103651	1.092	2	
	108046	1.171	3	
	112311	2.056	1	

Fig. 11. Vulnerability index result.

shows the VI in use, displaying results of the transformed data from Fig. 9 after being valued and clustered. As can be seen in Fig. 11, each polygon shows the different VV and cluster of the sample. The dendrogram heatmap is a visualization technique used to display the information developed by the clustering process. Due to the total case study having more than 130,000 debris locations, a random sample of 100 locations is shown on the map in which the 10 sample locations were taken. Each category shows individual metric severity in comparison with the same metric type of other locations. With every instance having a volume indicating the presence of debris, the most variation can be seen in the leftmost column of the dendrogram heatmap in Fig. 11. This map offers insight into metrics that disproportionately affect an area of analysis, but more so offers insight into which locations are clustered and share the most similar characteristics.

Based on the results found in Fig. 11, Polygon (instance) 49,037 is the most severe. Along with this, we can see that Cluster 1 contains the most severe values and would be the group of highest priority. An analysis of the Dendrogram Group 1 shows the most severe and varied volume and AADT values, which would be the like attributes that cause them to be clustered together. Clusters 4 and 5 are also similar, being primarily school and toxicity based. Cluster 3 only contains one location but is the only location with debris impeding an airport. This would allow for the removal of types of locations based on priority in this case starting at Polygon 49,037, then moving to 112,311, 60,509, 13,456, and last 6,339. This will allow decision makers to better equip removal teams and coordinate operations for removal and prioritize based on situational needs.

Limitations

Limitations of this research are present. This includes a lack of data, due to the small community mapping (data gathering) and low complexity of the area evaluated, the surrounding environment, and attributes from the other dimensions. The low data and complexity is the purpose of testing the complete framework and all dimensions on the larger and more complex nearby city of Corpus Christi. The second limitation stems from the operation of manually adding debris locations. Depending on the size of the region being evaluated without the aid of automation, the time required for data collection and processing could be extensive, depending on the level of detail desired. Due to the restricted nature of some registries needed for this study, a randomized format is used for the physical and environmental dimensions. The process and results of the data using the registries should not differ from the case study.

Conclusion

All communities fall at risk of the occurrence of a disaster hindering its ability to function. As shown a pre-disaster plan can greatly decrease the hindrance of debris on a community's ability to function. To aid in the post-disaster response to a community, the speed of removal has shown to have a direct impact on the safety of a community's citizens, its environment, and overall function. Pre-disaster planning has been shown to increase the effectiveness of the response phase, but with current deficiencies surrounding protocol, improvements to the current debris prioritization and removal process are needed to further aid the removal process. The purpose of the framework's systematic procedure is to aid in unifying the disaster response guidelines constructed by agencies that define best practice, and research that outlines innovation and areas of improvement. This framework was needed to create a platform for decision-makers in complex situations and give a resource to reduce decision-making and resource management.

The implementation of the three dimensions allowed for greater definition in the design of a disaster protocol and the accumulation of metric data. This also allows for a flexible metric system that can be readily adapted. Through the use of UAV and GIS mapping to derive data from existing resources, the transformation metrics allowed a user to cluster and prioritize locations. By applying the framework to areas such as those affected by Hurricane Harvey, the results showed the desired outcome of debris valued based on the formulated level of priority, with the visualization as intended. The results of the case study simulation show that the processing of an area and the effectiveness of evaluation of the area are consistent with the expected outcome established.

By evaluation of the VI from the sample of the 130,000 debris locations, represented in Fig. 11, shows that location vulnerability value is a good measure of severity based on polygon metrics. This is shown by location (polygon) 6339 being the least severe with a score of 0.900 and location 112311 as the most severe at 2.056. With this, clustering is also shown as a valuable means of organization. This is shown by the dendrogram in Fig. 11 grouping locations with similar metrics present being classed into the same cluster. Cluster 1 is the largest and primarily shows Volume and AADT metrics present, with Cluster 2 being the second largest and similar to Cluster 1 but including sever bridge metrics. This can be seen in all 5 clusters with all locations in each showing similar characteristics differentiating each cluster from the others.

The resulting Vulnerability Index provides a resource to decision-makers for greater information in a direct format that allows for improved decision-making in simple or complex environments. The three heatmaps developed and the available range of data visualization capabilities within each will allow decision-makers to make more effective decisions at a faster rate, allowing more focus on higher-impacted locations. This is accomplished by establishing severity values of metrics in each dimension and combining those for analysis of vulnerability and clustering.

The framework is meant to act as a base for a decision-maker that will work in any location and can be easily tailored to decision-makers needs by way of attribute expansion of metrics or clustering by different methods such as by layer or severity. Since all but the physical data is available pre-disaster, the only action to perform post-disaster is data collection and evaluation of the physical dimension. This process also serves as a platform for future research utilizing route optimization, temporary debris management site selection, and social media analysis. The improvements to the debris

removal process are established by a standardized framework to be applied to decision-making processes. In quantifying and ranking the severity of debris, stakeholders can focus on key dimensions that result in both clearer information and a reduced need for less important decision-making. The resulting heatmaps and index allow decision-makers to view and interpret the data in a variety of ways and to key in on areas that may be more heavily affected. They also allow for support systems to operate in a more effective, efficient, and safe manner during the response process, improving the disaster response scenario and, specifically, directly impacting the response phase of disaster relief.

Data Availability Statement

Some or all data, models, or code that support the findings of this study are available from the corresponding author upon reasonable request.

Acknowledgments

Data used were provided by A. Chang as part of the Texas A&M, Corpus Christi team.

References

Amadeo, K. 2019. "Hurricane Harvey facts, damage and costs." *The Balance*. Accessed January 2, 2022. https://www.lamar.edu/_files/documents/resilience-recovery/grant/recovery-and-resiliency/hurric2.pdf.

Barzilai, J., W. D. Cook, and B. Golany. 1992. "The analytic hierarchy process: Structure of the problem and its solutions." In *Systems and management science by extremal methods: Research honoring Abraham Charnes at age 70*, 361–371. Boston: Kluwer Academic.

Bhattacharyya, A., S. Yoon, T. J. Weidner, and M. Hastak. 2021. "Purdue Index for Construction analytics: Prediction and forecasting model development." *J. Manage. Eng.* 37 (5): 1–11. https://doi.org/10.1061/(ASCE)ME.1943-5479.0000944.

Blake, E. S., and D. A. Zelinsky. 2018. *Hurricane Harvey. National Hurricane Center tropical cyclone report*. Rep. No. NOAA/NWS AL092017. Washington, DC: National Oceanic and Atmospheric Administration.

Boin, A., and A. McConnell. 2007. "Preparing for critical infrastructure breakdowns: The limits of crisis management and the need for resilience." *J. Contingencies Crisis Manage.* 15 (1): 50–59. https://doi.org/10.1111/j.1468-5973.2007.00504.x.

Boyacı, B., and N. Geroliminis. 2012. "Facility location problem for emergency and on-demand transportation systems." In *Proc., 2012 Swiss Transport Research Conf. (STRC)*. Zürich, Switzerland: ETH Zürich.

Brock, S. E. 2018. *Descriptive statistics and psychological testing*. Long Beach, CA: California State Univ.

Brown, C., and M. Milke. 2009. *Planning for disaster debris management*. Christchurch, New Zealand: Univ. of Canterbury.

Carvalho, P. R., C. S. Munita, and A. L. Lapolli. 2019. "Validity studies among hierarchical methods of cluster analysis using cophenetic correlation coefficient." *Braz. J. Radiat. Sci.* 7 (2A): 1–14. https://doi.org/10.15392/bjrs.v7i2a.668.

Charrad, M., N. Ghazzali, V. Boiteau, and A. Niknafs. 2014. "Nbclust: An R package for determining the relevant number of clusters in a data set." *J. Stat. Software* 61 (6): 1–36. https://doi.org/10.18637/jss.v061.i06.

Chen, Y., and J. Yang. 2020. "Historic neighborhood design based on facility heatmap and pedestrian simulation: Case study in China." *J. Urban Plann. Dev.* 146 (2): 1–12. https://doi.org/10.1061/(ASCE)UP.1943-5444.0000554.

Crowley, J. 2017. "A measurement of the effectiveness and efficiency of pre-disaster debris management plans." *Waste Manage.* 62 (Apr): 262–273. https://doi.org/10.1016/j.wasman.2017.02.004.

Crowley, J., and P. Flachsbart. 2018. "Local debris management planning and FEMA policies on disaster recovery in the United States." *Int. J. Disaster Risk Reduct.* 27 (Jul): 373–379. https://doi.org/10.1016/j.ijdrr.2017.10.024.

Das, S., A. Bibeka, X. Sun, H. Zhou, and M. Jalayer. 2019. "Elderly pedestrian fatal crash-related contributing factors: Applying empirical bayes geometric mean method." *Transp. Res. Rec.* 2673 (8): 254–263. https://doi.org/10.1177/0361198119841570.

Da Silva, M. R., R. A. Eger, Y. A. Rosenfeldt, and C. Loch. 2018. "Testing DJI Phantom 4 Pro for urban georeferencing." *ISPRS Int. Arch. Photogramm. Remote Sens. Spatial Inf. Sci.* 42 (1): 407–411. https://doi.org/10.5194/isprs-archives-XLII-1-407-2018.

de Brito Neto, R. T., C. A. G. Santos, K. Mulligan, and L. Barbato. 2015. "Spatial and temporal water-level variations in the Texas portion of the Ogallala Aquifer." *Nat. Hazard.* 80 (1): 351–365. https://doi.org/10.1007/s11069-015-1971-8.

Duhamel, C., A. C. Santos, D. Brasil, E. Châtelet, and B. Birregah. 2016. "Connecting a population dynamic model with a multi-period location-allocation problem for post-disaster relief operations." *Ann. Oper. Res.* 247 (2): 693–713. https://doi.org/10.1007/s10479-015-2104-1.

EPA (Environmental Protection Agency). 2019a. *Managing your hazardous waste: A guide for small business*. Washington, DC: EPA. https://doi.org/10.4324/9781003008873-41.

EPA (Environmental Protection Agency). 2019b. *Planning for natural disaster debris*. Washington, DC: EPA.

EPA (Environmental Protection Agency). 2022. *Superfund chemical data matrix (SCDM) methodology.* Washington, DC: EPA.

e Silva, L. D., V. M. Alves, E. R. Dantas, L. Scotti, W. S. Lopes, E. N. Muratov, and M. T. Scotti. 2021. "Chemical safety assessment of transformation products of landfill leachate formed during the Fenton process." *J. Hazard. Mater.* 419 (Oct): 126438. https://doi.org/10.1016/j.jhazmat.2021.126438.

Fahad, M. G. R., W. C. Zech, R. Nazari, and M. Karimi. 2022. "Developing a geospatial framework for severe occupational injuries using Moran's I and Getis-Ord Gi* statistics for southeastern United States." *Nat. Hazard. Rev.* 23 (3): 1–12. https://doi.org/10.1061/(ASCE)NH.1527-6996.0000566.

FEMA. 2007. *Public assistance: Debris management guide*. Washington, DC: FEMA.

FEMA. 2017. *Pre-disaster recovery planning guide for local governments pre-disaster recovery planning guide for local governments*. Washington, DC: FEMA.

FEMA. 2019a. *FEMA grants $24 million for debris removal*. Washington, DC: FEMA.

FEMA. 2019b. *National response framework*. Washington, DC: FEMA.

FEMA. 2020a. *Emergency management in the United States—What are four phases of emergency.* Washington, DC: FEMA.

FEMA. 2020b. *Public assistance program and policy guide*. Washington, DC: FEMA.

Flenniken, J. M., S. Stuglik, and B. V. Iannone. 2020. "Quantum GIS (QGIS): An introduction to a free alternative to more costly GIS platforms." *Edis* 2020 (2): 7. https://doi.org/10.32473/edis-fr428-2020.

Ford, D. N., and C. M. Wolf. 2020. "Smart cities with digital twin systems for disaster management." *J. Manage. Eng.* 36 (4): 04020027. https://doi.org/10.1061/(ASCE)ME.1943-5479.0000779.

Forina, M., C. Armanino, and V. Raggio. 2002. "Clustering with dendrograms on interpretation variables." *Anal. Chim. Acta* 454 (1): 13–19. https://doi.org/10.1016/S0003-2670(01)01517-3.

FRCOG (Franklin Regional Council of Governments). 2014. *Franklin county disaster debris management plan*. Greenfield, MA: FRCOG.

GAO (US Government Accountability Office). 2016. *Information technology: FEMA needs to address management weaknesses to improve its systems*. Report to Congressional Requesters, GAO-16-306. Washington, DC: GAO.

Gu, Z. 2022. "Complex heatmap visualization." *IMeta* 1 (3): 1–15. https://doi.org/10.1002/imt2.43.

Gu, Z., R. Eils, and M. Schlesner. 2016. "Complex heatmaps reveal patterns and correlations in multidimensional genomic data." *Bioinformatics* 32 (18): 2847–2849. https://doi.org/10.1093/bioinformatics/btw313.

Guan, W., Q. Liu, and C. Dong. 2022. "Risk assessment method for industrial accident consequences and human vulnerability in urban areas." *J. Loss Prev. Process Ind.* 76 (Jan): 104745. https://doi.org/10.1016/j.jlp.2022.104745.

Gupta, S. 2013. "Using artificial neural network to predict the compressive strength of concrete containing nano-silica." *Civ. Eng. Archit.* 1 (3): 96–102. https://doi.org/10.13189/cea.2013.010306.

Huang, D., S. Wang, and Z. Liu. 2021. "A systematic review of prediction methods for emergency management." *Int. J. Disaster Risk Reduct.* 62 (Nov): 102412. https://doi.org/10.1016/j.ijdrr.2021.102412.

Hunter, J. E., and M. A. Hamilton. 2002. "The advantages of using standardized scores in causal analysis." *Hum. Commun. Res.* 28 (4): 552–561. https://doi.org/https://doi.org/10.1111/j.1468-2958.2002.tb00823.x.

Ismail Bin, M., and U. Dauda. 2013. "Standardization and its effects on K-means clustering algorithm." *Res. J. Appl. Sci. Eng. Techn.* 6 (17): 3299–3303. https://doi.org/10.19026/rjaset.6.3638.

Jeon, J., S. Padhye, S. Yoon, H. Cai, and M. Hastak. 2021. "Identification of metrics for the Purdue Index for Construction using latent Dirichlet allocation." *J. Manage. Eng.* 37 (6): 1–13. https://doi.org/10.1061/(ASCE)ME.1943-5479.0000968.

Kim, J. 2014. "A framework of effective debris management for a resilient community." Doctoral dissertation, Dept. of Civil Engineering, Purdue Univ.

Kim, J., A. Deshmukh, and M. Hastak. 2018. "A framework for assessing the resilience of a disaster debris management system." *Int. J. Disaster Risk Reduct.* 28 (Dec): 674–687. https://doi.org/10.1016/j.ijdrr.2018.01.028.

Kohlitz, J., J. Chong, and J. Willetts. 2020. "Rural drinking water safety under climate change: The importance of addressing physical, social, and environmental dimensions." *Resources* 9 (6): 77. https://doi.org/10.3390/resources9060077.

Lauritzen, E. K. 2018. "Disaster waste management guidelines." In *Construction, demolition and disaster waste management*, 203–273. Boca Raton, FL: CRC Press. https://doi.org/10.1201/b20145-6.

Liu, K., Z. Yuan, X. Xin, J. Zhang, and W. Wang. 2021. "Conflict detection method based on dynamic ship domain model for visualization of collision risk hot-spots." *Ocean Eng.* 242 (Feb): 110143. https://doi.org/10.1016/j.oceaneng.2021.110143.

Lorca, Á., M. Çelik, Ö. Ergun, and P. Keskinocak. 2015. "A decision-support tool for post-disaster debris operations." *Procedia Eng.* 107 (Jan): 154–167. https://doi.org/10.1016/j.proeng.2015.06.069.

Lorca, Á., M. Çelik, Ö. Ergun, and P. Keskinocak. 2017. "An optimization-based decision-support tool for post-disaster debris operations." *Prod. Oper. Manage.* 26 (6): 1076–1091. https://doi.org/10.1111/poms.12643.

Luther, L. 2006. *Disaster debris removal after Hurricane Katrina: Status and associated issues*. Washington, DC: Congressional Research Service.

Marchesini, G., and B. Barroca. 2021. "Quantification of disaster waste: Review of the available methods." *Int. J. Disaster Risk Reduct.* 53 (Feb): 101996. https://doi.org/10.1016/j.ijdrr.2020.101996.

McNeill, L. H., M. W. Kreuter, and S. V. Subramanian. 2006. "Social environment and physical activity: A review of concepts and evidence." *Soc. Sci. Med.* 63 (4): 1011–1022. https://doi.org/10.1016/j.socscimed.2006.03.012.

Milligan, G. W., and M. C. Cooper. 1988. "A study of standardization of variables in cluster analysis." *J. Classif.* 5 (2): 181–204. https://doi.org/10.1007/BF01897163.

Murtagh, F., and P. Contreras. 2011. "Methods of hierarchical clustering." Preprint, submitted April 30, 2011. https://arxiv.org/abs/1105.0121.

Naderpajouh, N., J. Choi, and M. Hastak. 2016. "Exploratory framework for application of analytics in the construction industry." *J. Manage. Eng.* 32 (2): 1–11. https://doi.org/10.1061/(ASCE)ME.1943-5479.0000409.

National Research Council. 1994. "Ranking hazardous-waste sites for remedial action." In *Ranking hazardous-waste sites for remedial action*. Washington, DC: National Academies Press. https://doi.org/10.17226/4781.

Nevill, A. M., G. Atkinson, M. D. Hughes, and S. M. Cooper. 2002. "Statistical methods for analysing discrete and categorical data recorded in performance analysis." *J. Sports Sci.* 20 (10): 829–844. https://doi.org/10.1080/026404102320675666.

Nielsen, F. 2016. *Introduction to HPC with MPI for data science*. Cham, Switzerland: Springer.

Nkikabahizi, C., W. Cheruiyot, and A. Kibe. 2022. "Chaining Z-score and feature scaling methods to improve neural networks for classification." *Appl. Soft Comput.* 123 (Jul): 108908. https://doi.org/10.1016/j.asoc.2022.108908.

Paton, D., L. Smith, and J. Violanti. 2000. "Disaster response: Risk, vulnerability and resilience." *Disaster Prev. Manage. Int. J.* 9 (3): 173–180. https://doi.org/10.1108/09653560010335068.

Patro, S. G. K., and K. K. Sahu. 2015. "Normalization: A preprocessing stage." Preprint, submitted March 19, 2015. https://arxiv.org/abs/1503.06462.

Sansone, S. M., A. Schneider, E. Bickel, E. Berry-Kravis, C. Prescott, and D. Hessl. 2014. "Improving IQ measurement in intellectual disabilities using true deviation from population norms." *J. Neurodev. Disord.* 6 (Dec): 1–5. https://doi.org/10.1186/1866-1955-6-16.

Saraçli, S., N. Doğan, and I. Doğan. 2013. "Comparison of hierarchical cluster analysis methods by cophenetic correlation." *J. Inequal. Appl.* 2013 (1) :1–8. https://doi.org/10.1186/1029-242X-2013-203.

Schwab, B., S. Janzen, N. P. Magnan, and W. M. Thompson. 2020. "Constructing a summary index using the standardized inverse-covariance weighted average of indicators." *Stata J.* 20 (4): 952–964. https://doi.org/10.1177/1536867X20976325.

Siebert, S., and J. Teizer. 2014. "Mobile 3D mapping for surveying earthwork projects using an unmanned aerial vehicle (UAV) system." *Autom. Constr.* 41 (May): 1–14. https://doi.org/10.1016/j.autcon.2014.01.004.

TCS (Thompson Consulting Services). 2017. *Debris removal report*. Maitland, FL: TCS.

Tran, D. Q., M. Park, D. Jung, and S. Park. 2020. "Damage-map estimation using UAV images and deep learning algorithms for disaster management system." *Remote Sens.* 12 (24): 4169. https://doi.org/10.3390/rs12244169.

Truong, L. T., and S. V. C. Somenahalli. 2011. "Using GIS to identify pedestrian-vehicle crash hot spots and unsafe bus stops." *J. Public Transp.* 14 (1): 99–114. https://doi.org/10.5038/2375-0901.14.1.6.

Tseng, J. M., T. S. Su, and C. Y. Kuo. 2012. "Consequence evaluation of toxic chemical releases by ALOHA." *Procedia Eng.* 45 (Jan): 384–389. https://doi.org/10.1016/j.proeng.2012.08.175.

TxDOT (Texas Department of Transportation). 2022. *Open data portal*. Austin, TX: TxDOT.

UNEP (United Nations Environment Programme). 2008. *Disaster waste management mechanism*. Nairobi, Kenya: UNEP.

UN (United Nations). 2015. *Disaster preparedness for effective response*. San Francisco: United Nations.

UN (United Nations). 2017. *Flash Environmental Assessment Tool (FEAT)*. San Francisco: United Nations.

USAF (US Army Forces). 1999. *Domestic emergencies handbook*. 2nd ed. Fayetteville, NC: US Army Forces Command Domestic Plans Branch.

USCB (United States Census Bureau). 2020. *Data set: Area & population*. Washington, DC: US Department of Commerce.

USDOT. 2020. *Emergency response guidebook*. Washington, DC: USDOT. https://doi.org/10.1201/b22284-14.

Van Pham, H., and P. Moore. 2019. "Emergency service provision using a novel hybrid SOM-spiral STC model for group decision support under dynamic uncertainty." *Appl. Sci.* 9 (18): 3910. https://doi.org/10.3390/app9183910.

Violán, C., A. Roso-Llorach, Q. Foguet-Boreu, M. Guisado-Clavero, M. Pons-Vigués, E. Pujol-Ribera, and J. M. Valderas. 2018. "Multimorbidity patterns with K-means nonhierarchical cluster analysis."

BMC Fam. Pract. 19 (1): 1–11. https://doi.org/10.1186/s12875-018-0790-x.

Yeom, J., Y. Han, A. Chang, and J. Jung. 2019. "Hurricane building damage assessment using post-disaster UAV data." In *Proc., Int. Geoscience and Remote Sensing Symp. (IGARSS), 2019-July*, 9867–9870. New York: IEEE. https://doi.org/10.1109/IGARSS.2019.8900477.

Yoon, D. K. 2012. "Assessment of social vulnerability to natural disasters: A comparative study." *Nat. Hazards* 63 (2): 823–843. https://doi.org/10.1007/s11069-012-0189-2.

Yoon, S., J. Jeon, H. Cai, and M. Hastak. 2021. "Verification and validation framework for Purdue Index for Construction." *J. Manage. Eng.* 37 (1): 1–12. https://doi.org/10.1061/(ASCE)ME.1943-5479.0000850.